Graded-threshold parametric response maps: towards a strategy for adaptive dose painting

A Lausch[1], N Jensen[2], J Chen[3], TY Lee[1], M Lock[3], E Wong[1,2]

[1] Department of Medical Biophysics, The University of Western Ontario, London, ON, N6A 3K7, Canada

[2] Department of Physics and Astronomy, The University of Western Ontario, London, ON, N6A 3K7, Canada

[3] London Regional Cancer Program, London, ON, N6A 4L6, Canada

Email: alausch2@uwo.ca

Purpose: To modify the single-threshold parametric response map (ST-PRM) method for predicting treatment outcomes in order to facilitate its use for guidance of adaptive dose painting in intensity-modulated radiotherapy.

Methods: Multiple graded thresholds were used to extend the ST-PRM method (Nat. Med. 2009;15(5):572-576) such that the full functional change distribution within tumours could be represented with respect to multiple confidence interval estimates for functional changes in similar healthy tissue. The ST-PRM and graded-threshold PRM (GT-PRM) methods were applied to functional imaging scans of 5 patients treated for hepatocellular carcinoma. Pre and post-radiotherapy arterial blood flow maps (ABF) were generated from CT-perfusion scans of each patient. ABF maps were rigidly registered based on aligning tumour centres of mass. ST-PRM and GT-PRM analyses were then performed on overlapping tumour regions within the registered ABF maps.

Main findings: The ST-PRMs contained many disconnected clusters of voxels classified as having a significant change in function. While this may be useful to predict treatment response, it may pose challenges for identifying boost volumes or for informing dose-painting by numbers strategies. The GT-PRMs included all of the same information as ST-PRMs but also visualized the full tumour functional change distribution. Heterogeneous clusters in the ST-PRMs often became more connected in the GT-PRMs by voxels with similar functional changes.

Conclusions: GT-PRMs provided additional information which helped to visualize relationships between significant functional changes identified by ST-PRMs. This may enhance ST-PRM utility for guiding adaptive dose painting.

1. Introduction

Traditionally, the aim of radiation therapy (RT) is to deliver a large homogeneous dose of radiation to the tumour while limiting the dose to surrounding critical structures. With intensity modulated radiation therapy (IMRT) and image-guidance dose can be delivered with more conformality and precision than ever before. This has led to significant interest in the idea of using non-homogeneous dose distributions to take advantage of heterogeneity in tumour radio-sensitivity. This concept has been termed "dose-painting" and involves the use of functional imaging as a surrogate for indicating tumour radio-sensitivity or risk of relapse after treatment [1]. Approaches have typically involved

delivering boost doses to predicted radio-resistant tumour sub volumes or heterogeneous doses to the entire tumour which scale with local radio-resistance ("dose-painting-by-numbers") [1].

Recently, Galban et al [2] have demonstrated a promising new method for predicting treatment outcomes which may be well-suited towards informing dose painting techniques. Parametric response maps (PRMs) are generated which indicate whether each tumour voxel has undergone a significant increase or decrease in function as indicated by analysis of functional imaging acquired before and during treatment. This information was found to be predictive of overall survival among a cohort of patients treated for glioma and imaged with perfusion MRI [1]. Therefore tumour response and progression could potentially have been visualized during treatment on a voxel-by-voxel basis using the PRMs. Consequently the PRM method may be ideal for informing adaptive dose painting techniques within contexts in which its predictive utility has been verified.

To date, the PRM method has been investigated within a few different contexts [2-5]. Galban et al. are currently investigating the use of a PRM biomarker to identify non-responding patients treated for glioma who might benefit from salvage therapy with bevacizumab and dose painting IMRT [6]. However, these results are not yet available and to our knowledge no other studies discussing the PRM method as applied to dose painting have appeared in the literature.

The PRM method employs a single threshold value to distinguish if tumour functional changes are significant with respect to treatment outcomes. In this study we present a natural extension of this method which uses multiple graded thresholds in order to improve PRM utility within adaptive dose painting contexts. Hereafter the original and proposed PRMs are referred to as single-threshold PRMs (ST-PRM) and graded-threshold PRMs (GT-PRM) respectively. We motivate and discuss the underlying logic of GT-PRMs by comparing them to traditional ST-PRMs through application of both methods to CT-perfusion scans of patients treated with RT for hepatocellular carcinoma.

2. Materials and methods

2.1. Single-threshold parametric response maps

To generate ST-PRMs, baseline functional imaging acquired before treatment is compared to followup imaging acquired during treatment. Since the comparison is voxel-based, the scans must be spatially aligned using image registration. A tumour voxel is classified as significantly increasing or decreasing in function if its functional change (ΔF) is such that $\Delta F > +T$ or $\Delta F < -T$ respectively, where T is a single threshold value. Voxels for which $|\Delta F| \leq T$ are classified as "insignificant change". ST-PRMs correspond to images of the tumour that indicate which voxels significantly increased, decreased, or did not significantly change in function after treatment.

T is determined by the functional changes observed within similar healthy tissue [2]. Here, the ST-PRM thresholds were determined by investigating the functional changes in the remaining healthy portions of the liver. The function of each healthy liver voxel in the followup scan is plotted against the function of each corresponding voxel in the baseline scan. $[-T, T]$ is then defined to be the 95% confidence interval for the residuals that result from fitting a line to this plot. Consequently, changes in tumour function are considered to be significant if they exceed the magnitude of most of the changes observed in similar healthy tissue that is untreated.

2.2. Graded-threshold parametric response maps

GT-PRMs are generated in much the same way as ST-PRMs except multiple thresholds are used in order to classify voxels by the magnitude of their functional changes. Let $\{T_i\}$ for $i = 1...10$ represent a set of thresholds. Each $[-T_i, T_i]$ corresponds to a different confidence interval for the residuals from the same plot used to determine the threshold for the original PRM method. In this study, the T_i for $i = 1...10$ corresponded to the 5%, 15%, 25%, 35%, 45%, 55%, 65%, 75%, 85%, and 95% confidence intervals respectively. Accordingly, T_{10} is the same threshold used to generate the ST-PRMs

To create the GT-PRM, each tumour voxel is classified by the maximum threshold that its associated functional change exceeds. This classification is represented visually by assigning a value

of $\pm i$ to each voxel in the map where $+i$ indicates $\Delta F > +T_i$ and $-i$ indicates $\Delta F < -T_i$. For example, a value of 5 indicates that $T_5 \leq \Delta F < T_6$ whereas a value of -5 indicates $-T_6 < \Delta F \leq -T_5$.

2.3. Example cases
The abdominal CT-perfusion scans of 5 patients with hepatocellular carcinoma were used for this study. Scans were acquired pre and post-RT using a 64 slice scanner (Discovery VCT or CT750HD, GE Healthcare, Waukesha, WI) with a spatial resolution of 0.7 mm by 0.7 mm by 5 mm and a temporal resolution of 2.8 seconds. Each image volume contained 512x512x16 voxels. Arterial blood flow (ABF) functional image maps were generated from each 4D acquisition.

2.4. Image registration
To estimate ST-PRM and GT-PRM thresholds, the healthy liver must be accurately aligned within the pre and post-RT ABF maps. The average pre and post-RT 4DCT scans were non-rigidly registered to one another using an elastic, spline-based, multi-resolution registration algorithm [7]. The resulting transformations were then used to align the pre and post-RT ABF functional maps.

While the above method is suitable for registering the healthy liver, its accuracy cannot be assumed within the tumour region due to potential volume changes that are unrelated to motion. Consequently ST-PRM and GT-PRM analysis was performed on rigidly registered ABF maps instead of the non-rigidly registered maps used for threshold estimation. The tumours were delineated in the pre and post-RT scans and then rigidly registered by aligning their centers of mass. Subsequent analysis was performed only on the overlapping regions of the tumour within the rigidly registered maps. This approach is similar to Galban et al [2].

3. Results and discussion
ST-PRM and GT-PRM maps were computed and then superimposed on the associated average pre-RT 4DCT for each patient (Figure 1). For further comparison, maps indicating the relative difference in tumour ABF (RD-ABF) were also generated. RD-ABF was defined as the difference between the pre and post-RT voxels divided by the magnitude of the maximum ABF difference within the tumour.

The ST-PRMs contained many disconnected clusters of voxels that were classified as significantly increasing or decreasing in function. Since a single threshold is used to determine functional change significance, ST-PRMs do not contain information regarding the lesser magnitude functional changes within the voxels surrounding these disconnected clusters. While surrounding voxels may not be predictive of outcomes, their values help to visualize the spatial functional change relationships between the disconnected clusters of significantly changing voxels. Since GT-PRMs are generated using multiple thresholds they can convey this information along with all of the ST-PRM information.

For example, the ST-PRM for patient 4 contains a large circular sub region with mostly insignificant functional changes and some significant increases (red) and decreases (blue) speckled throughout. However, the GT-PRM indicates that these clusters are connected by voxels that are mostly increasing in function with many of the changes exceeding the T_5 (55% CI) threshold. This demonstrates a systemic regional functional increase which may be useful for defining a radiation boost volume for adaptive radiotherapy. Similarly for the other ST-PRMs, regional functional change relationships become clearer within the corresponding GT-PRMs.

The RD-ABF maps also provided insight into regional functional change relationships. However the GT-PRMs illustrate this information while putting it into context with respect to the changes that might be expected due to normal physiological variation. The observer can immediately identify and stratify the potential treatment related significance of tumour functional changes. Therefore, GT-PRMs may be amenable to informing adaptive dose-painting-by-numbers whereby local tumour dose is scaled by the significance of local functional changes.

In this study, pre and post-RT ABF maps were used to demonstrate the GT-PRM method. As a result of treatment or progression related tumour volume changes, registration may have been less accurate within the tumours. In practice, followup imaging would be acquired during treatment
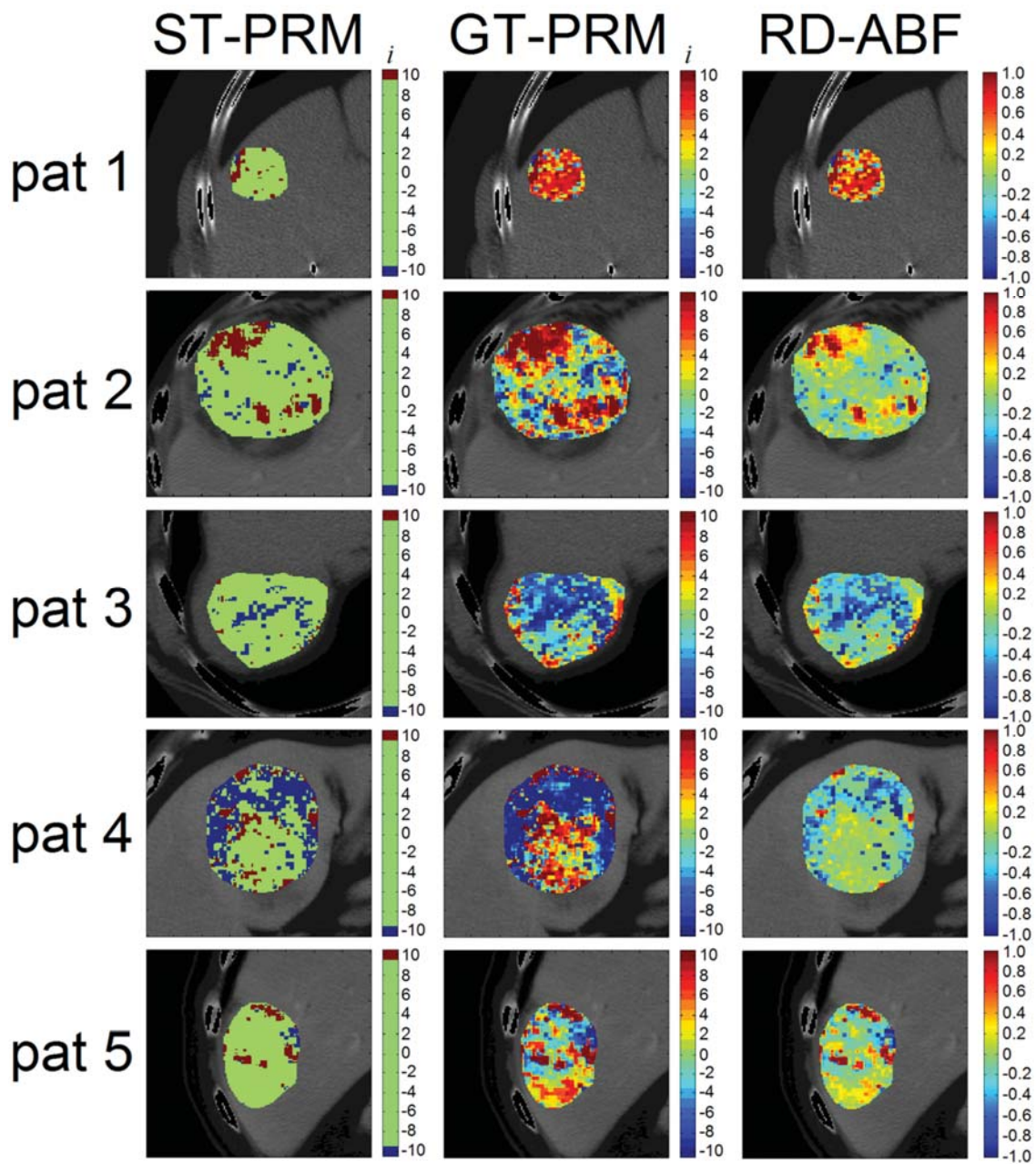
Figure 1. Representative slice from patient 3 simulations. Maps were cropped down to a 10x10 cm field of view and values outside the tumour were suppressed for improved visualization. A) S_0P_3 and S_iP_3 (no RE), B) $S_iP_3M_8$ (~4.3 mm average RE) and C) $S_iP_3M_{20}$ (~7.5 mm average RE)

reducing volume changes and associated registration uncertainty. Registration errors could lead to tumour voxel misclassification for both the ST-PRM and GT-PRM methods. However, the severity of misclassification within GT-PRMs should be reduced since a spectrum of graded thresholds are employed. For example, a significantly increasing voxel misclassified as unchanging by a ST-PRM, could be misclassified as a somewhat less significantly increasing voxel in a GT-PRM rather than completely unchanging. Consequently, GT-PRMs may be more robust to registration error with respect to visualization of regional functional change relationships.

Ultimately, the predictive utility of the PRM method needs to be verified for each combination of imaging modality and pathology. This work has not yet been done for liver tumours. Liver tumour examples were selected within the present study for several reasons. First, due to RT delivery constraints, dose-painting by numbers or delivering boosts to tumour subvolumes may only be feasible in larger tumours. Liver tumours referred for RT tend to be large and unresectable, and therefore potentially amenable to this treatment approach. Second, prognosis for patients with liver tumours remains poor [8] and so there is a push to develop new treatment techniques which offer improved outcomes. In principle, the ST-PRM and GT-PRM methods can be applied to any pathology with repeat imaging. In the absence of verified predictive utility, the GT-PRM still provides an effective means of visualizing functional changes with respect to estimated normal physiological variations.

4. Conclusion

The ST-PRMs contained many disconnected clusters of voxels classified as having a significant change in function. While this may be useful to predict global treatment response, it may pose challenges for identifying boost volumes or for informing dose-painting by numbers strategies. The GT-PRMs included all of ST-PRM information but also visualized the full tumour functional change distribution. GT-PRMs provided additional information which helped to visualize relationships between significant functional changes identified by ST-PRMs. This may enhance PRM utility for guiding adaptive dose painting.

References
[1]   Bentzen S M, Gregoire V. 2011 *Semin. Radiat. Oncol.* **21** 101-10
[2]   Galban C J et al. 2009 *Nature Medicine* **15**(5) 572-76
[3]   Galban C J et al. 2009 *Transl. Oncol.* **2**(3) 184-90
[4]   Hoff B A et al. 2012 *Bone* **51**(1) 78-84
[5]   Harris R J, Cloughesy T F, Pope W B, Nghiemphu PL, Lai A, Zaw T, Czernin J, Phelps ME, Chen W, Ellingson BM. 2012 *Neuro-Oncology* **14**(8) 1079-89
[6]   Galban C J et al. 2011 *Clin. Cancer. Res.* **17**(14) 4751-60
[7]   Modersitzki J 2009 *FAIR: Flexible Algorithms for Image Registration*. Philadelphia, USA: Society for Industrial and Applied Mathematics.
[8]   Ellison LF, Wilkins K. 2010 *Health Reports* **21**(3) 55-60